Phase transformations in Fe–Cr–Mn alloys for magnetocaloric applications

X. Hai, Charlotte Mayer, Sophie Tencé, Salvatore Miraglia

Phase transformations in Fe-Cr-Mn alloys for magnetocaloric applications

X. Hai[1,2], C. Mayer[2], S. Tencé[3] ,S. Miraglia[1*]

(1) Université Grenoble Alpes, CNRS, Institute NEEL, 25 rue des Martyrs, 38042 Grenoble

(2) Erasteel SAS, Tour Montparnasse, 33 avenue du Maine F-75015 Paris

(3) CNRS, Univ. Bordeaux, ICMCB, UPR 9048, 87 avenue du Dr A. Schweitzer, F-33608 Pessac

(*) corresponding author

Abstract

The sequence of phase transformations in a Fe-Cr-Mn alloy (known as an austenitic stainless steel) are investigated in order to explore the potential of this rare earth-free material for magnetocaloric applications at high temperature. In the lack of high temperature X-ray diffraction the magnetic response and transition temperatures of alloys have been determined by using a Faraday's Balance apparatus and an extraction vector magnetometer. These characterizations have been complemented by DCS and DTA measurements as well as thermodynamic calculations using Thermocalc. The retained nominal composition is $Fe_{0.59}Cr_{0.16}Mn_{0.25}$ (referred to as FeCrMn 15/25) shows the targeted reversible transformation. Carbon addition is shown to shift the transition temperature to lower values. The effect of carbon addition on the phase transition and on the magnetocaloric response is discussed.

A comparison is made with the chromium-poor Fe-Cr-Ni system.

Keywords : austenitic steels, magnetocaloric effect

1. Introduction

The magnetocaloric effect (MCE) is the change in temperature of a material due to the adiabatic application or removal of an external magnetic field. This temperature change is related to the magnetic entropy change (ΔS_M). Generally, MCE is large in the vicinity of the Curie temperature (T_C), where the magnetic spins undergo an order - disorder phase transition. Historically this effect found its application for cooling in low temperature physics by using the

adiabatic demagnetization of paramagnetic salts in 1933 [1]. The study of room temperature MCEs associated with a magnetic phase transition was revived in 1997 by Pecharsky and Gschneidner [2] who observed a 'giant' entropy change in $Gd_5Si_2Ge_2$. From then on, the MCE has been considered for room temperature refrigeration technology using materials with a transition near room temperature or for heat-to-power conversion, where an appropriate thermodynamic cycle is chosen to use the magnetocaloric material for power generation.

Today, a large set of magnetic materials show significant magnetocaloric effects. Most of such materials contain rare earths. In order to be considered for application, the magnetocaloric material should be sustainable and environmentally-friendly. Considering the fact that the economic and strategic issues surrounding rare earths are very complex, there exists a motivation to find novel rare earth free magnetocaloric materials. In particular there is a considerable interest in rare earth free, cost effective and readily available Fe-based materials. This paper intends to investigate the potential of some Fe-based alloys for magnetocaloric applications. A literature review, summarized in the next section, prompted us to investigate the Fe-Cr-Mn system which has not been reported so far.

2 State of the art

Among the Fe-containing alloys, Fe_xPt_{100-x} alloys exhibit a temperature and magnetic field induced phase transition from disordered γ phase to ordered α phase. This gives rise to a magnetic entropy change up to 39.8 J/kg. K for alloy $Fe_{79}Pt_{21}$ under a field change of 0 to 7 T [3]. Their magnetocaloric effect near room temperature makes Fe_xPt_{100-x} alloys interesting candidates for magnetic refrigeration applications. Nonetheless, the price of Pt remains a challenge for the upscaling of these alloys.

In 2012, P. Souvatzis and colleagues [4] reported a theoretical prediction to achieve a structural and magnetic phase transition in alloy systems $Fe_{1-y-x}Cr_yNi_x$ and $Fe_{1-y-x}Cr_yMn_x$ where $0.1<y<0.3$ and $0.1<x<0.3$. They predicted that it was possible to tune the composition so that the bcc to fcc phase transition took place in a temperature range close to room temperature, accompanied with a large change in entropy of the spin-system. By alloying with Ni or Mn, the ferromagnetic bcc-phase of $Fe_{1-y}Cr_y$ ($y < 20$) can degenerate with the paramagnetic fcc-phase [5, 6]. As the ferrite bcc-phase is being heated, it becomes destabilized and results in transforming into the paramagnetic fcc-phase at the transition temperature [6]. This structural and magnetic transition is expected to be accompanied by a large entropy change. Therefore, it should be possible to tailor the bcc to fcc transformation with the composition and microstructure engineering.

Some authors have used ball milling to synthesize nanocrystalline powder of Fe-Ni alloys. Ipus and co-workers have shown that γ-FeNi nanoparticles exhibit a near room-temperature second-order magnetocaloric response [7]. The peak entropy change is in the order of 2.8 J/kg·K for a maximum applied field of 5 T.

Later in 2013, Ucar and colleagues studied mechanically alloyed $Fe_{70}Ni_{30}$ and $Fe_{72}Ni_{28}$ and characterized them in terms of their structural and magnetic properties [8]. The maximum magnetic entropy change observed for $Fe_{70}Ni_{30}$ and $Fe_{72}Ni_{28}$ are 0.65 and 0.5 J/kg·K, respectively, at a field of 5 T. The peak temperatures are around 90 and 60 °C, respectively. The Curie temperature of these nanoparticles were tuned by controlling the oxidation kinetics of Fe during ball milling. The Fe-Ni phase diagram shows that the magnetic properties and Curie temperature of these alloys strongly depend on the composition. Chaudhary *et al.* reported the magnetocaloric effect and magnetic properties of $(Fe_{70}Ni_{30})_{95}Mn_5$ nanoparticles prepared by ball milling [9]. The quenched sample shows a Curie temperature at 65 °C. They show that the maximum entropy change is 1.45 J/kg·K for a field change of 5T.

A multiphase Fe-Ni-B bulk alloy has been investigated as a solution for inadequate temperature span in developing a magnetic cooling system [10]. The bcc phase forms during slow cooling from the fcc phase region to room temperature in the furnace. The coexistence of bcc, fcc, and spinel phases results in large working temperature spans of 439 °C for magnetic field change of 5 T. The mass fraction of the phases can be tuned by controlling the synthesis parameters.

Likewise, MCE in cementite (Fe_3C) has been explored in a recent publication by B. Kaeswurm *et al.* [11]. While the transition temperature (202 °C) is still high for room-temperature magnetic refrigeration, the material has a measured magnetocaloric effect of ΔT_{ad} = 1.76 K and ΔS = 3 J/kg·K for a field change from 0 to 2 T. The Curie temperature of cementite can be adjusted by substitution of various elements. For instant, small concentration of Molybdenum can reduce T_C from 202 °C down to 147 °C [12]. Other variations have been examined, including $(Fe_{0.9}Mn_{0.1})_3C$, with a reported ΔS of 3.4 J/kg·K at 32 °C for a field change of 5 T, and $Fe_{2.85}Cr_{0.05}C$ [12], which crystallizes in the cementite type structure and shows a temperature-induced second-order magnetic phase transition at 87 °C.

3 Experimental details

After preliminary studies, Fe-Cr-Mn alloys selected for this study have been prepared by high-frequency induction melting ultra-pure elemental compounds in appropriate nominal

compositions. Carbon insertion was performed via a solid-solid reaction with an intermediate alloy. The as-cast alloys were then wrapped in Mo foil and sealed in quartz ampoule, filled with partial pressure of argon. Annealing was performed for 15 days at 1000 ˚C. The magnetic response and transition temperatures of alloys were determined by a Faraday's Balance apparatus and an extraction vector magnetometer. Calorimetric measurements were carried out using Differential Scanning Calorimeter (DSC) in the range from room temperature to 800 °C and Differential Thermal Analysis (DTA) from room temperature to 1300 °C. The sample mass for the measurement is about 100 mg and pure Al_2O_3 is used as a reference material. Qualitative information on the phase presence given by X-ray diffraction at room temperature using a PANalytical X'Pert MRD X-ray diffractometer operated at the Cu K_α wavelength. Metallographic characterization was done by optical and electronic microscopes with appropriate chemical attack of the surface. Since the alloying elements are all neighboring elements with very similar atomic number, the accurate composition of the different phases was difficult to obtain in EDX analysis. The magnetization measurements were performed by using a high-temperature VSM. The isothermal magnetic entropy change was obtained from isothermal magnetization measurements from 50 K below the transition temperature to 50 K above the transition temperature with a temperature step size of 3K and a field variation from 0 to 20 kOe. Knowing that this indirect method leads to the estimation that depends on the measuring procedure, we used a protocol in which, after each temperature step, the sample is cooled from its paramagnetic state before starting a new isothermal measurement.

4 Results and discussion

Only α-ferrite and α'-martensite phases are known to possess ferromagnetic properties at and above room temperature. The respective transition temperatures depend on the composition of the phases. In order to evaluate a large range of compositions, several alloys with different Cr, Ni, and Mn content were synthesized and characterized in the $Fe_{1-x-y}Cr_xNi_y$ (Cr wt%=5,15,25,35 and Ni wt%=10,15,20,25) and $Fe_{1-x-y}Cr_xMn_y$ (Cr wt%=5,15 and Mn wt%=10,20,25) systems respectively. The compositions were selected on the basis of Thermocalc predictions and phase diagrams in order to position near the two-phase (bcc and fcc) region. The TCFE6 database is specifically applicable for various types of steels/Fe-alloys with a minimum Fe-content of 50 wt%. The database has been based on complete reassessments of binary and many ternary systems; however, many intermediate compounds that do not occur in steels/Fe-alloys have been deleted from the database. Therefore, it is not suitable to calculate complete binary and

ternary systems, but rather only in the iron-rich corner (in our case the iron content is 65wt%). In this study, the pressure in the simulated system is set to standard atmospheric condition and the system size is 1 mole.

These thermodynamic simulations are used to predict stability phases within a certain temperature range as a reference to the experimental data and to select viable compositions to test experimentally. In addition, the ThermoCalc simulations cannot provide information on the kinetics of phase transformation. Experimentally, the system is not in equilibrium during heating and cooling so this needs to be taken into consideration. Therefore phase fractions from Thermocalc cannot be directly compared with DSC figures. In this paper, we focus on results from $Fe_{0.59}Cr_{0.16}Mn_{0.25}$ (Fe65Cr15Mn25) due to the possible relevance in magnetocaloric application. The other compositions were found to exhibit disappointingly low MCEs and are therefore not reported, those results may be found in [13]. A shorthand notation of 15/25 is used in the following section to refer to this Fe-based alloy with 15 wt%Cr and 25 wt%Mn.

4.1 Alloy 15/25

The phase formation is first simulated with Thermocalc© software with TCFE6 database. Based on the thermodynamic calculation (Figure 1) for alloy 15/25, austenite (γ-fcc) phase is the primary solidification phase, together with a small percentage of σ phase (20%). The ferrite phase starts to form below 500 °C. The σ phase is present both before and after the transformation between bcc and fcc phases.

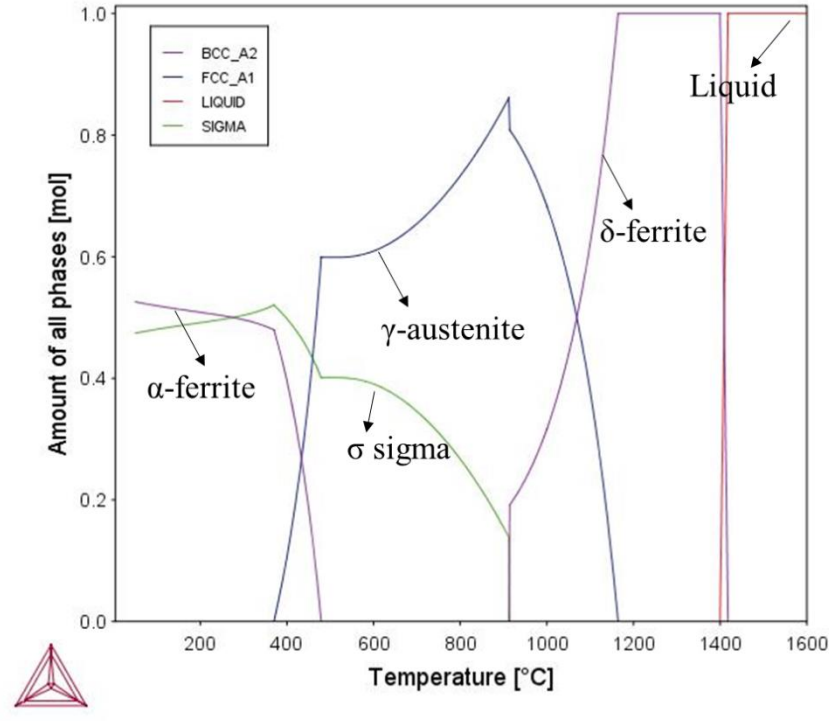

Figure 1. Phase fraction as a function of temperature for alloy 15/25 calculated using Thermocalc©.

The XRD pattern confirms that the sample contains a majority phase in a bcc structure with a Fe_7Ni_3-type lattice. The lattice parameter is about 2.86 Å. The microstructure of the annealed sample was observed in optical microscope after HNO_3 electrolytic etching on the surface. The microstructure shown in Figure 2 shows austenite phase with ferrite grains and small dark dots of sigma phase.

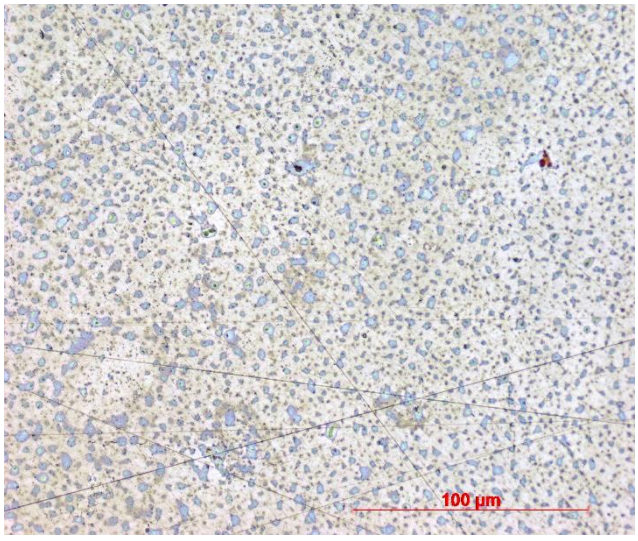

Figure 2. Microstructure after HNO_3 electrolytic etching for alloy 15/25 annealed at 1000 °C for 15 days.

The phase transition is examined by means of Faraday's balance and DSC. Figure 3 (a) shows a transition from a ferromagnetic ferrite phase to a paramagnetic austenite phase during heating for sample 15/25. The DSC measurements in figure 3b display a sluggish endothermic signal

in the temperature range [500°C-600°C] upon heating whereas no significant thermal event can be detected in the same temperature range upon cooling. For a first order phase transformation between equilibrium crystallographic phases (the common type) an endothermic heat effect will occur upon heating and the opposite effect is expected to occur during cooling. Our respective observations, magnetic (fig 3a) and calorimetric (fig 3b), are consistent with the following assumptions :

- a very sluggish structural transformation is likely to take place around 600°C
- since the ferromagnetic to paramagnetic transformation is a second order transformation no heat effect should accompany it, therefore the magnetic signal observed in fig. 3a is likely to be Curie point effect.

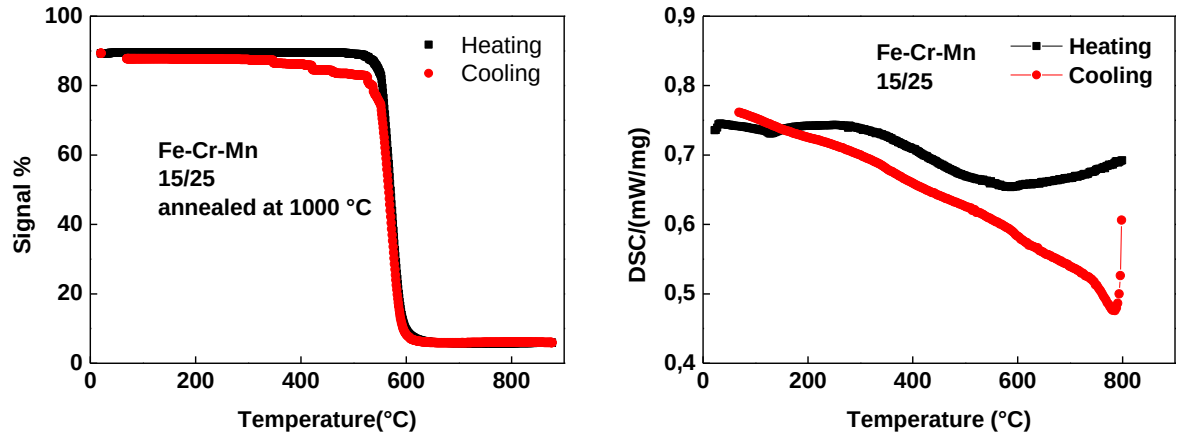

(a) *(b)*

Figure 3. (a) Magnetic response in arbitrary units for samples 15/25 and (b) DSC measurement for alloy 15/25.

In this α/γ material, we manage to find the reversible structural transformation inducing a magnetic transition, even though the transformation temperature is too high for room-temperature application. Alloy 15/25 was treated in thermal cycles to observe its cyclic behavior. The transition is quite stable from both (a) cycling with cooling to RT at each cycle and (b) cycling without cooling down to RT at each cycle, as shown in Figure 4.

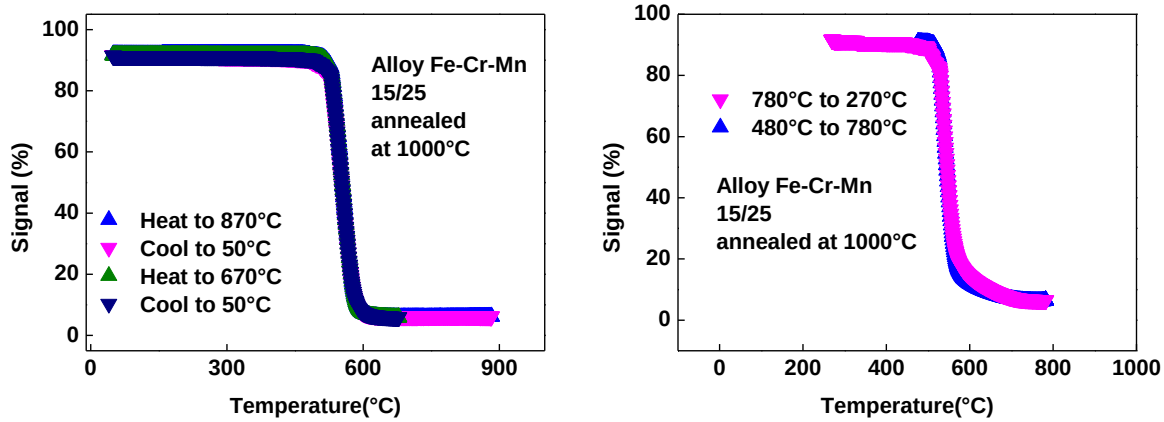

(a) Cycles cooling to RT *(b) Cycles without cooling to RT*

Figure 4. The magnetic response in arbitrary units of annealed sample 15/10 is plotted as a function temperature during (a) thermal cycles cooling down to RT at each cycle and (b) thermal cycles without going back to room temperature at each cycle

4.2 Effect of carbon addition

Carbon is one of the γ-promoting alloying elements, which means that the addition of carbon stabilizes the high temperature austenite phase, lowering the ferrite to austenite transition temperature. Seen from the previous section, sample 15/25 shows very little thermal hysteresis, which is an advantage to study the influence of carbon on the transition temperature. Different concentrations of carbon were added by induction melting graphite with the other starting elements in order to elaborate samples with 0.05, 0.1, and 0.2 wt% of C. We use the shorthand notations 15/25/0.05, 15/25/0.1, and 15/25/0.2 to distinguish the samples. The alloys were annealed at 1100 °C and then quenched

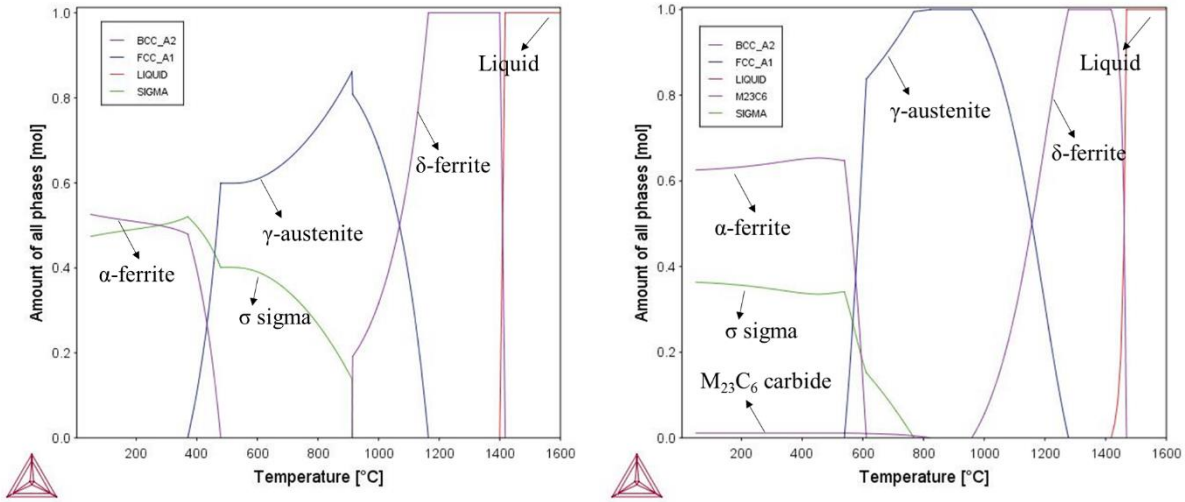

15/25 *15/25/0.05*

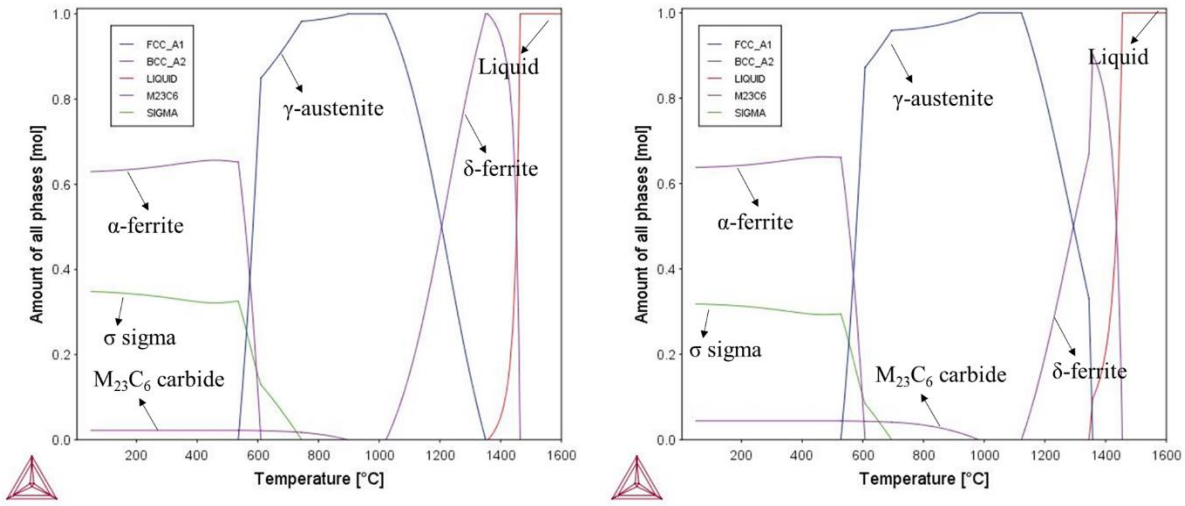

Figure 5. Thermodynamic calculations for alloy 15/25 and the carbonated samples.

As shown in the thermodynamic calculation (Figure 5), the sigma phase is stabilized at lower temperature with increasing carbon content. According to Thermocalc calculations (figure 5) the effects of carbon addition in the FeCrMn alloy are the following :

- A shrinking of the stability range of sigma phase which is no longer stable at temperatures above 600°C
- In the mean time the precipitation of $M_{23}C_6$ carbides is favoured
- Finally the transition between alpha-ferrite and gamma-austenite is shifted from 400°C for pristine alloy to about 600°C for C-doped ones

Our magnetic measurements (figure 6) show a lowering of magnetic transition from 600°C down to 400°C which does not further depend on the carbon content. These experimental observations are consistent with Thermocalc calculations for the pristine alloy. For this alloy the calculations predict the presence of austenite and sigma phase and the lack of ferrite above 600°C. At 400°C ferrite, sigma phase and austenite may coexist.

For the carbon-doped samples the calculations predict the presence of austenite, sigma phase, $M_{23}C_6$ carbide and the presence of ferrite at 600°C (boundary). At 400°C ferrite, sigma phase and $M_{23}C_6$ carbide may coexist. The weakness and/or lack of magnetic signal above 400°C is therefore inconsistent with the presence of ferrite above 400°C for the carbon-doped samples. The common austenitization process is a ferrite to austenite transformation accompanied by a dissolution of the $M_{23}C_6$ particles. Recently [14] the extent of interaction of Cr-rich carbides dissolution and the austenitic growth has been reassessed for Cr-containg steels (our case). It was found that small carbide paticle size promote faster austenite transformation leading to ferrite-free microstrucures at lower temperatures (because of kinetics effects). Therefore our current experimental observations (figure 6) are consistent with such a scenario.

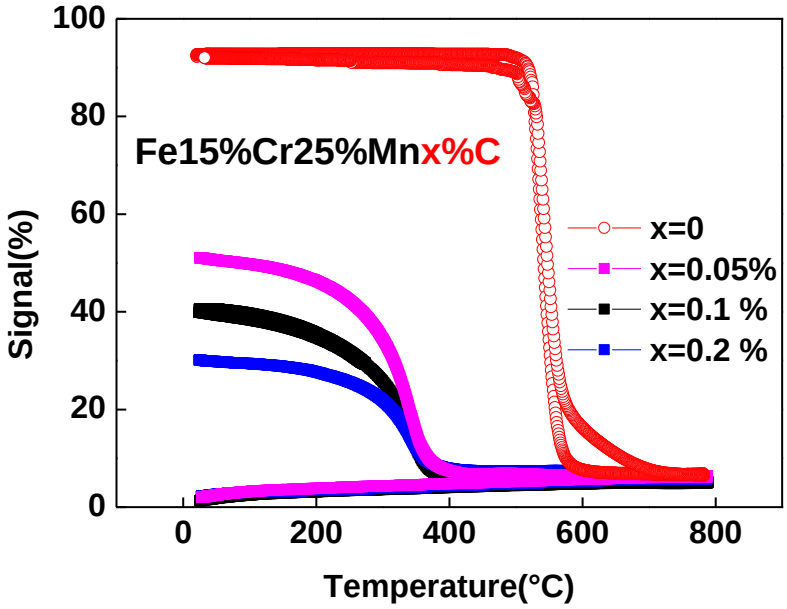

Figure 6. Magnetic response in arbitrary units for sample $Fe_{0.59}Cr_{0.16}Mn_{0.25}$ and the carbon-doped counterparts.

Since the magnetic signals from the Faraday's balance are qualitative only, the magnetization level of the carbon-containing alloys has been further verified using an extraction vector magnetometer. The magnetization level decreases with increasing carbon content. Alloy 15/25/0.05 has a magnetization value of 31.36 $A \cdot m^2/kg$ and for alloy 15/25/0.1, this value is dropped to 20.35 $A \cdot m^2/kg$. The paramagnetic behavior upon cooling of some carbonated samples also suggests the presence of sigma or carbide phases. The martensite starting temperatures calculated for these samples are all below 0 °C, which explains the absence of the recovering of martensite phase upon cooling.

The transition temperature for sample 15/25/0.1 is 362 °C. (see figure 7a) and displays a small hysteresis. The magnetization loop shown in Figure 7 (b) illustrates the soft magnetic behavior of the sample.

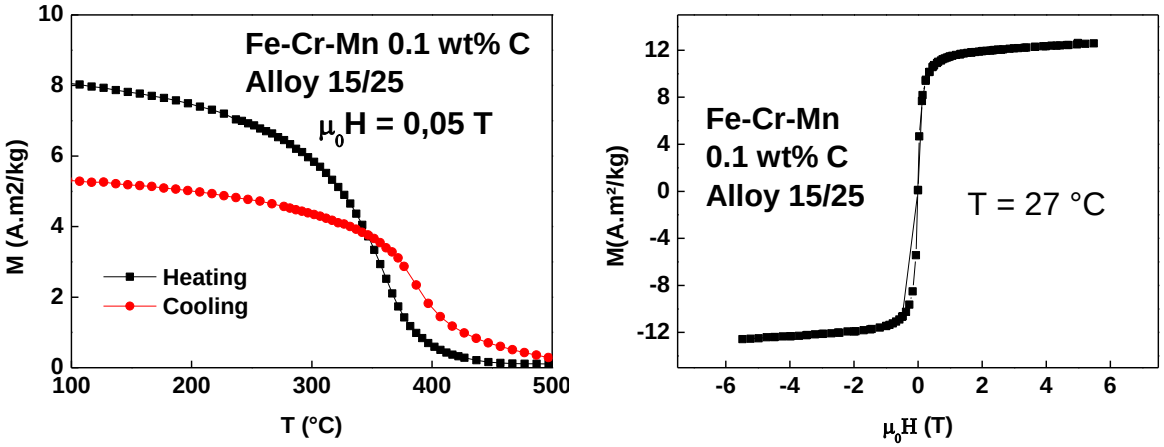

(a) H = 0.05 T *(b) T = 300 K*

Figure 7. (a) Magnetization as a function of temperature under constant field of 0.05 T for sample 15/25/0.1 and (b) magnetization as a function of field at 300 K.

4.3 Magnetocaloric characterization

Figure 8 shows the temperature dependence of the magnetic entropy change under a magnetic field ranging from 0 to 2O KOe. It can be seen that carbon addition resulted in a shift of the transition temperature to lower values but the measured entropy change is very low and out of consideration for any application. The non-doped alloy instead, exhibits an entropy change comparable to that of chromium-doped Fe70Ni30 nanoparticles [15] at the corresponding magnetic field change. Such composition is therefore suitable for high temperature cooling.

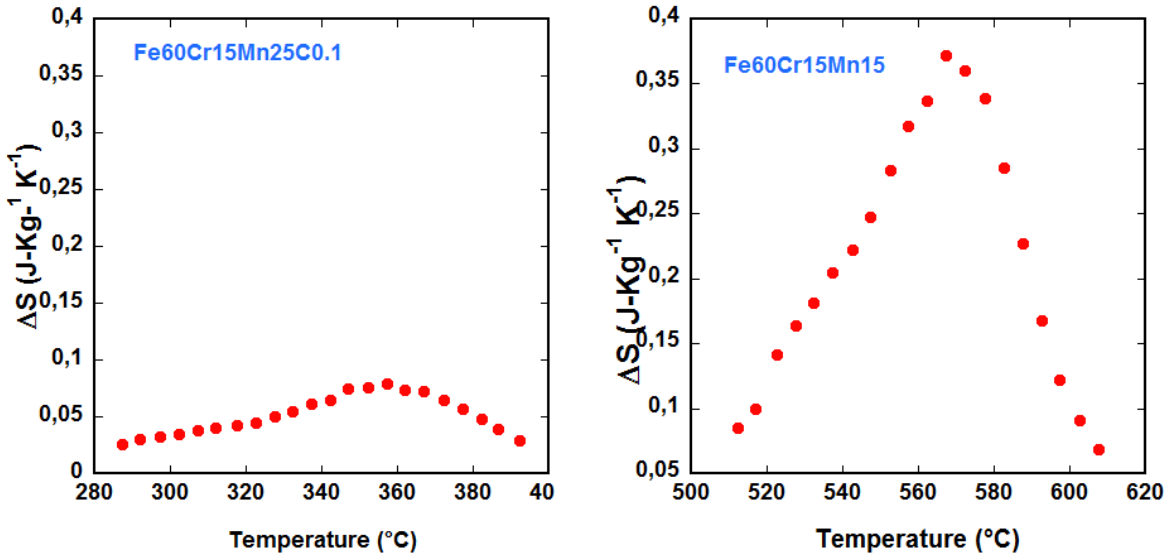

Figure 8. Magnetic entropy change dependence on temperature for sample 15/25/0.1 and 15/25

It is our contention that there exists a solicitation in regard to the development of compact, low weight magnetic refrigerators that can operate at high temperatures. Development of such systems would allow for a more local, and more efficient, cooling process. The primary initial market opportunity for such magnetocaloric refrigeration systems would be for systems where localized cooling at high temperatures is required.

5 Conclusion

The Fe-Cr-Mn alloy 15/25 shows the targeted reversible structural transformation between ferrite and austenite, but this transformation occurs around 550-600°C and the trials with C doping did not allow to decrease this transition temperature while maintaining a large magnetic change and a reversible transformation.

The carbon addition to Fe-Cr-Mn alloy 15/25 can effectively decrease the transition temperature from ferrite to austenite during heating. However, this is accompanied by a change of structural transitions in the sample. The carbon-containing alloys show bcc to fcc transition upon heating.

However, the Mn and C concentrations further stabilize austenite phase, which is not transformed into ferrite upon cooling. Therefore, carbon alloying has compromised the reversibility of the magneto-structural transition observed in 15/25 alloy.

Acknowledgements

This work was supported by the CIFRE Project No.2013/0827.

Highlights

Low cost austenitic steels

Rare earth-free magnetocaloric materials

High temperature solid state cooling

Graphical Abstract

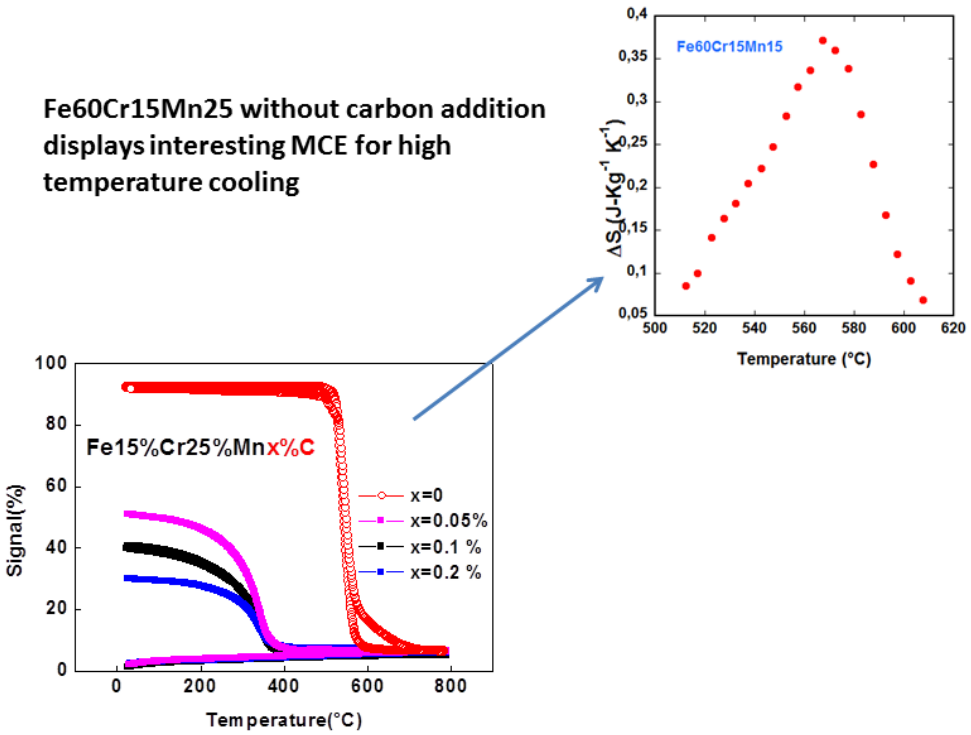

References

[1] W. F. Giauque and D. P. MacDougall, Phys. Rev. 43, 768 (1933).

[2] V. K. Pecharsky and K. A. Gschneidner, Jr., Phys. Rev.Lett. 78, 4494, (1997).

[3] C. Rong et J. Liu, *Appl. Phys. Lett.*, vol. 90, p. 222504, 2007.

[4] P. Souvatzis, L. Vitos et O. Eriksson, *Cond. Mat. Mtrl. Sci.*, p. 15, 2012.

[5] A. Majumdar et P. Blanckenhagen, *Phys. Rev. B*, vol. 29, p. 4079, 1984.

[6] M. Acet, T. Schneider et E. Wassermann, *J. Phys. IV C2-105, supp. J. Phys. III*, vol. 5, 1995.

[7] J. J. Ipus, H. Ucar et M. E. McHenry, *IEEE Trans. Magn.*, vol. 47, n° %110, p. 2494, 2011.

[8] H. Ucar, J. J. Ipus, D. E. Laughlin et M. E. McHenry, *J. Appl. Phys.*, vol. 113, p. 17A918, 2013.

[9] V. Chaudhary, A. Chaturvedi, I. Sridhar et R. V. Ramanujan, *IEEE Magn. Lett.*, vol. 5, p. 6800104, 2014.

[10] V. Chaudhary et R. V. Ramanujan, *IEEE Magn. Lett.*, vol. 6, p. 6700104, 2015.

[11] B. Kaeswurm, K. Friemert, M. Gürsoy, K. Skokov et O. Gutfleisch, *J. Magn. Magn. Mater.*, vol. 410, p. 105, 2016.

[12] T. Sato, T. Nishizawa et K. Tamaki, *Trans. JIM*, vol. 3, p. 196, 1962.

[13] X. Hai, "Magnetocaloric materials for room temperature refrigeration," Ph.D. dissertation (Université Grenoble Alpes 2016).

[14] A.M. Bettanini, L. Ding, J.D. Mithieux, C. Parrens, H. Idrissi, D. Schryvers, L. Delannay, T. Pardoen, T. Jacques Materials and Design 162 (2019) 362-374

[15] Chaudhary, V. and Ramanujan, R.V. Magnetocaloric Properties of Fe-Ni-Cr Nanoparticles for Active Cooling. *Sci. Rep.* **6**, 35156; doi: 10.1038/srep35156 (2016).)